Collective emission in Dirac structures

Konstantin Batrakov

Research Institute for Nuclear Problems, Belarusian State University, Minsk 220030, Belarus

Grodno, Belarus, August 12-24, 2018

The XIV-th International School-Conference

The Actual Problems of Microworld Physics

In Memory of Professor Nikolai Shumeiko

OUTLINE

- Very brief introduction to Dirac- (Weil-) type materials
- Some examples of Dirac (Weyl) materials.
- Our results concerning collective emission
- Conclusions

EXAMPLES OF DIRAC STRUCTURES

Graphene

single layer of graphite, firstly exfoliated in 2005, nowadays can be produced be means of chemical vapor deposition (Nobel prize in Physics 2010, Geim and K.Novoselov)

Topological insulators

$Bi_{1-x}Sb_x$(alloy), Bi_2Se_3, Bi_2Te_3, $TlBiSe_2$, $TlBiTe_2$, strained HgTe

Hsieh, D., Qian, D., Wray, L., Xia, Y., Hor, Y. S., Cava, R. J. and Hasan, M. Z. (2008), A topological Dirac insulator in a quantum spin Hall phase, Nature 452, 970–974;
T.O. Wehling, A.M. Black-Schaffer & A.V. Balatsky, Dirac materials, Advances in Physics, 63(1) ,1 (2014) doi 10.1080/00018732.2014.927109;
G. Tkachov, Topological Insulators: The Physics of Spin Helicity in Quantum Transport (Pan Stanford Publishing 2015, 182 p.

Weyl semimetals

TaAs, Weil type fermion was first experimentally discovered in 2015.

Massless Dirac (Weyl) hamilonian

$$\hat{H} = v\boldsymbol{\alpha}\mathbf{p}$$

In the Weyl representation :

$$\boldsymbol{\alpha} = \begin{pmatrix} \boldsymbol{\sigma} & 0 \\ 0 & -\boldsymbol{\sigma} \end{pmatrix}$$

Consequence of Dirac-Weyl system dynamics is Klein “paradox” and particle tunneling with high transmittance through barrier with $V_0 > 2m$.

The basis of generation in graphene and nanotubes

1) The possibility of strong electromagnetic wave slowing down [G. Ya. Slepyan, S. A. Maksimenko, A. Lakhtakia, O. Yevtushenko, A. V. Gusakov, Phys. Rev. B 60, 17136 (1999)].

2) Ballistic electron transport (up to tens of μm) [C. Berger, P. Poncharal, Y. Yi, W. A. de Heer,J. Nanosci. Nanotechn., 3, 171 (2003)]; Jens Baringhaus, Ming Ruan, Frederik Edler, & Walt A. de Heer *Nature* **506**, 349–354, 20 February 2014 doi:10.1038/nature12952

3) Very large current density (up to 10^{10} A/cm^2) [M. Radosavljevi´c, J. Lefebvre, and A. T. Johnson, Phys. Rev. B 64, 241 307® (2001); S.-B. Lee, K. B. K. Teo, L. A. W. Robinson, A. S. Teh, M. Chhowalla, et al., J. Vac. Sci. Technol. B 20, 2773 (2002)];

ČERENKOV LASING IN CNT

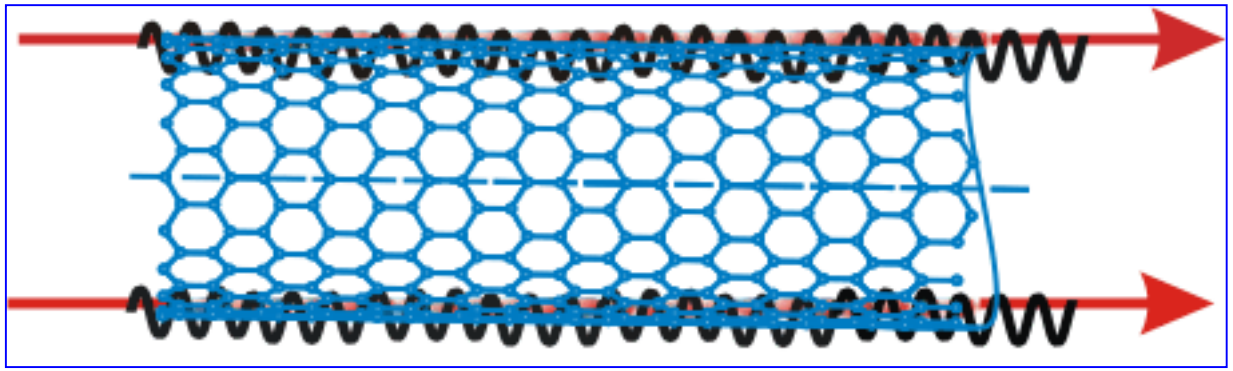

K. G. Batrakov, P. P. Kuzhir, S. A. Maksimenko, *Proc.SPIE 6328, 63280Z (2006)*
K. G. Batrakov, S. A. Maksimenko, P. P. Kuzhir, and C. Tomsen, *Phys. Rev. B 79, 125408 (2009).*
K.G. Batrakov, O.V. Kibis, Polina P. Kuzhir, M. R. Costa, and M. E. Portnoi, Vol. **4**, 041665 (2010).
.

Threshold current and radiative instability increment

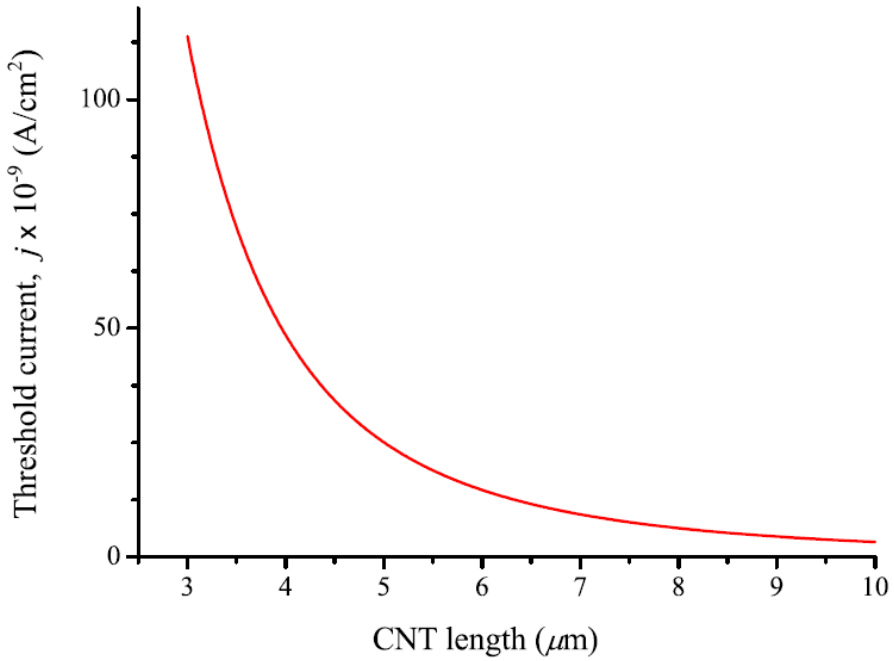

FIG. 4. (Color online) The dependence of threshold current density on nanotube length.

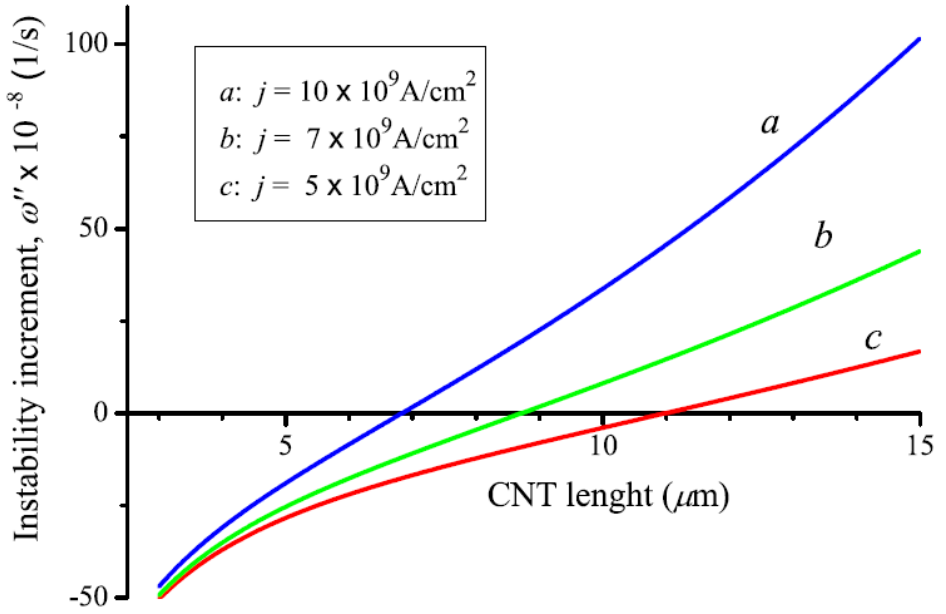

FIG. 5. (Color online) Instability increment vs nanotube length at different electron current densities.

Figures from paper:

K. G. Batrakov, S. A. Maksimenko, P. P. Kuzhir, and C. Tomsen, *Phys. Rev. B 79, 125408 (2009)*

Advantage of using two-wall, multiwall nanotube or graphene for emission

Estimated wave retardation in single walled nanotube reach 50 times. It is not enough for

For long wavelength $\lambda >> d$ (d is the distance between nanotube layers), frequencies may be approximately written as: $\omega_+ \sim \omega_1(R_1)+\omega_2(R_2)$ and $\omega_- \sim |\omega_1(R_1)-\omega_2(R_2)|$

Phase velocity corresponding to frequency $\omega_-, v_{ph-} = \omega_- / k$ *can be significantly less, than phase velocities corresponding to single walled nanotubes* !!! However $\omega_1(R_1) \neq \omega_2(R_2)$ *, therefore decreasing of phase velocity in two-wall nanotube is limited.*

Bilayer graphene has no such drawback?..... But it turns out that phase velocity in bilayer graphene exceeds phase velocity in graphene monolayer. Electron tunneling between graphene layers **is guilty**.

Tunneling should be suppressed.

It can be realized in spatially separated double-layer or multilayer graphene.

K. Batrakov, V. Saroka, S. Maksimenko, Chr. Thomsen, Journal of Nanophotonics, **6**, 061719 (2012)

Graphene sandwich

PMMA (poly(methyl methacrylate)

Graphene

Two spatially separated graphene monolayers (2-layer sandwich)

Solution of boundary problem with boundary conditions on graphene layers gives dispersion equation for eigen waves

$$\mathbf{H}(z_i+0)-\mathbf{H}(z_i-0)=\frac{4\pi}{c}[\mathbf{j}_t(z_i)\times\mathbf{n}]$$ - discontinuity magnetic field on opposite sides of graphene sheet

Dispersion equation for surface TM mode in two-layer graphene system

$$2+\frac{4\pi}{c}\sigma\frac{k_z c}{\omega}\pm\frac{4\pi}{c}\sigma\frac{k_z c}{\omega}\exp\{-\sqrt{q^2-\omega^2/c^2}\,l\}=0$$

Here q is wave vector , $k_z=\sqrt{\omega^2/c^2-q^2}$, l is distance between graphene layers

Graphene sheet conductance:

$$\sigma^{\text{intra}}(\omega,\mu,T,\gamma_{\text{trans}})=\frac{e^2 g_s g_v}{16\hbar}\frac{8T}{\pi\hbar}\ln\left|2\cosh\left(\frac{\mu}{2T}\right)\right|\frac{i}{\omega+i\gamma_{\text{trans}}}$$

$$\sigma^{\text{inter}}(\omega,\mu,T,\gamma_{\text{opt}})=-\frac{ie^2 g_s g_v}{16\pi\hbar}\tilde{\Omega}\int_0^\infty\frac{\sinh(x|\mu|/T)}{\cosh(\mu/T)+\cosh(x\mu/T)}\frac{dx}{x^2-\tilde{\Omega}^2/4}$$

$\tilde{\Omega}=\hbar(\omega+i\gamma_{\text{opt}})/|\mu|$, μ is chemical potential, γ_{trans} γ_{opt} are broadening parameters.

Symmetric mode. Frequency tuning by varying of chemical potential.

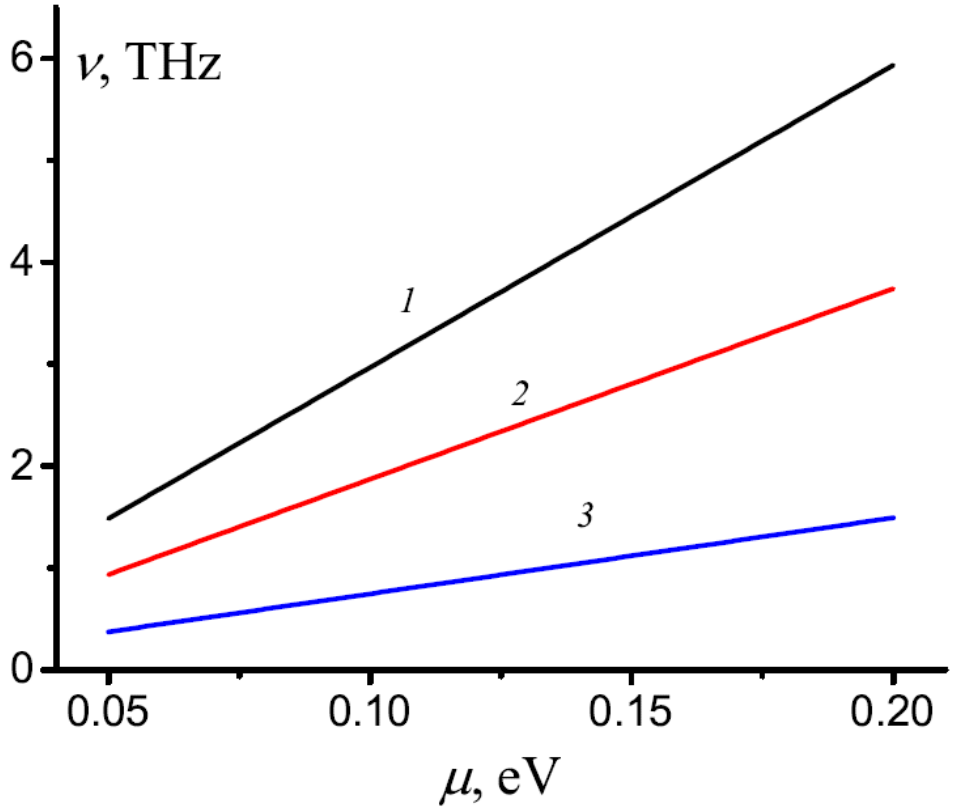

Čerenkov resonant frequency vs chemical potential at the electron beam energy 4 KeV (1),
10 KeV (2) and 60 KeV (3).

Chemical potential can be tuned by:
1) Electrostatic doping (smooth frequency tuning); 2) by number of layers, because in “+” mode potential is proportional to this number (discrete tuning)

Asymmetric mode. Strong wave slowing down. Tuning by graphene interlayer distance variation

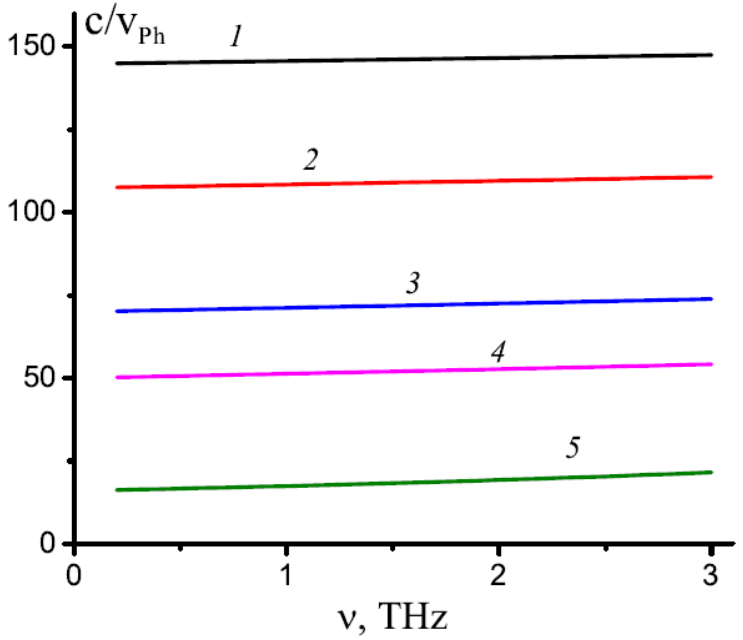

Phase velocity slowing down for the asymmetric mode in structure with two graphene layers.
In curves 1 - 4, the distances between layers are 20 nm, 50 nm, 100 nm and 1 μm, respectively.
Chemical potential in all cases is 0.1 eV.

$$\sigma' = \frac{e^2}{\hbar} g_s g_v \frac{T}{\pi\hbar} \log\left[2\cosh\left(\frac{\mu}{2T}\right)\right] \frac{i\omega_{tr}}{\omega_{tr} + (\omega_{tr}^2 - v_F^2 q^2)^{1/2}} \frac{1}{(\omega_{tr}^2 - v_F^2 q^2)^{1/2}} \qquad \omega_{tr} = \omega + i\gamma_{trans}$$

Hybrid modes in three-layered graphene sandwich

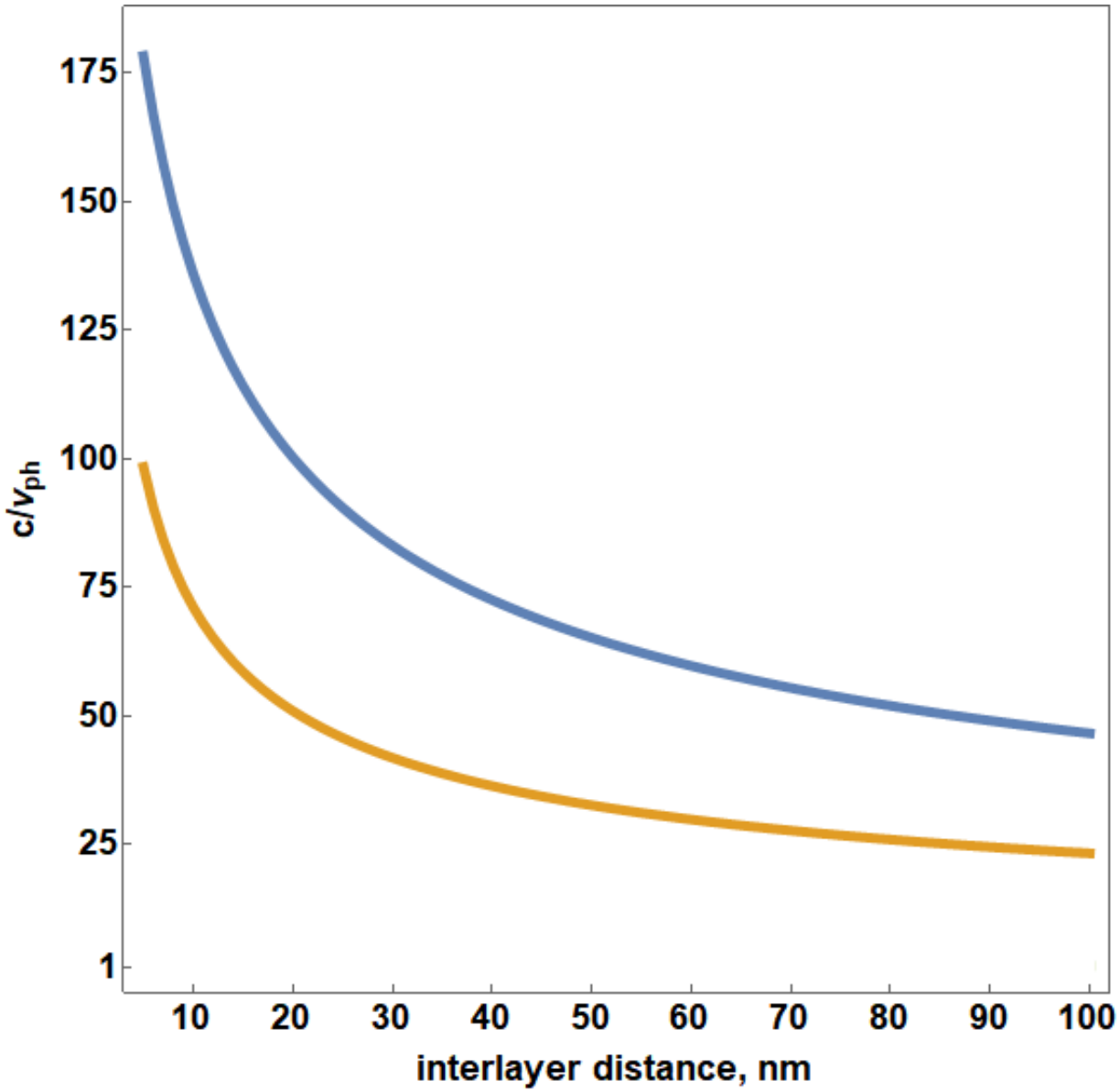

$$\mu_{eff} = 2T \log\left[2\cosh\left(\frac{\mu}{2T}\right)\right]$$

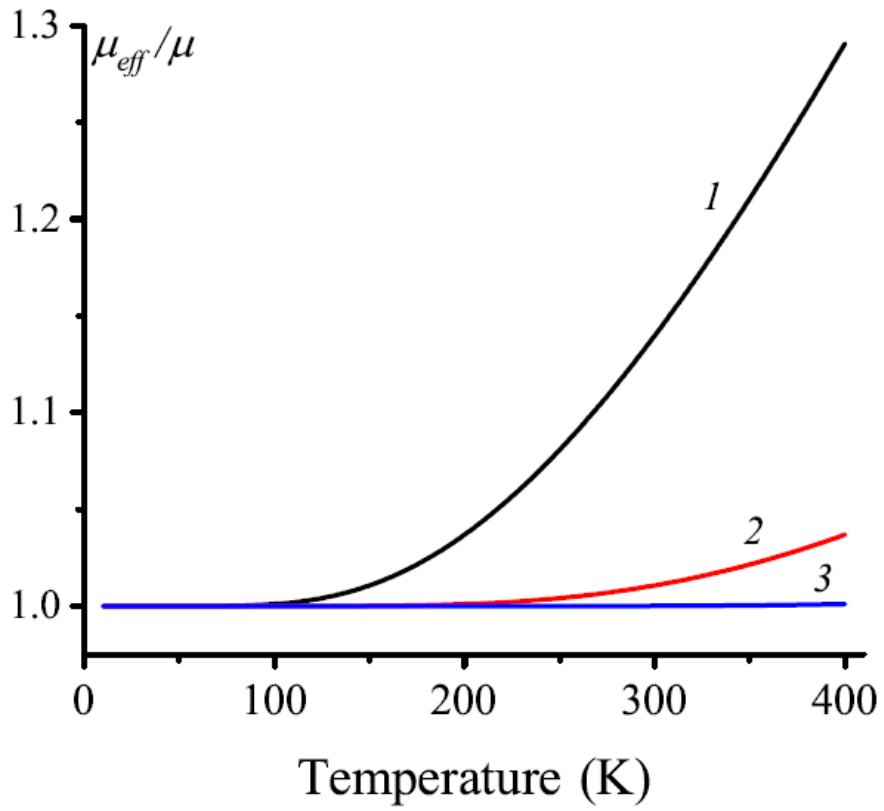

FIG. 7: Temperature dependence of the effective chemical potential for different values of chemical potential: $\mu = 0.05$(curve *1*), 0.1 (curve *2*), 0.2 (curve *3*)

Figure from the paper: K. Batrakov and S. Maksimenko, Graphene layered systems as a terahertz source with tuned frequency. Phys. Rev. B 95, 205408 (2017)

Čerenkov generation scheme

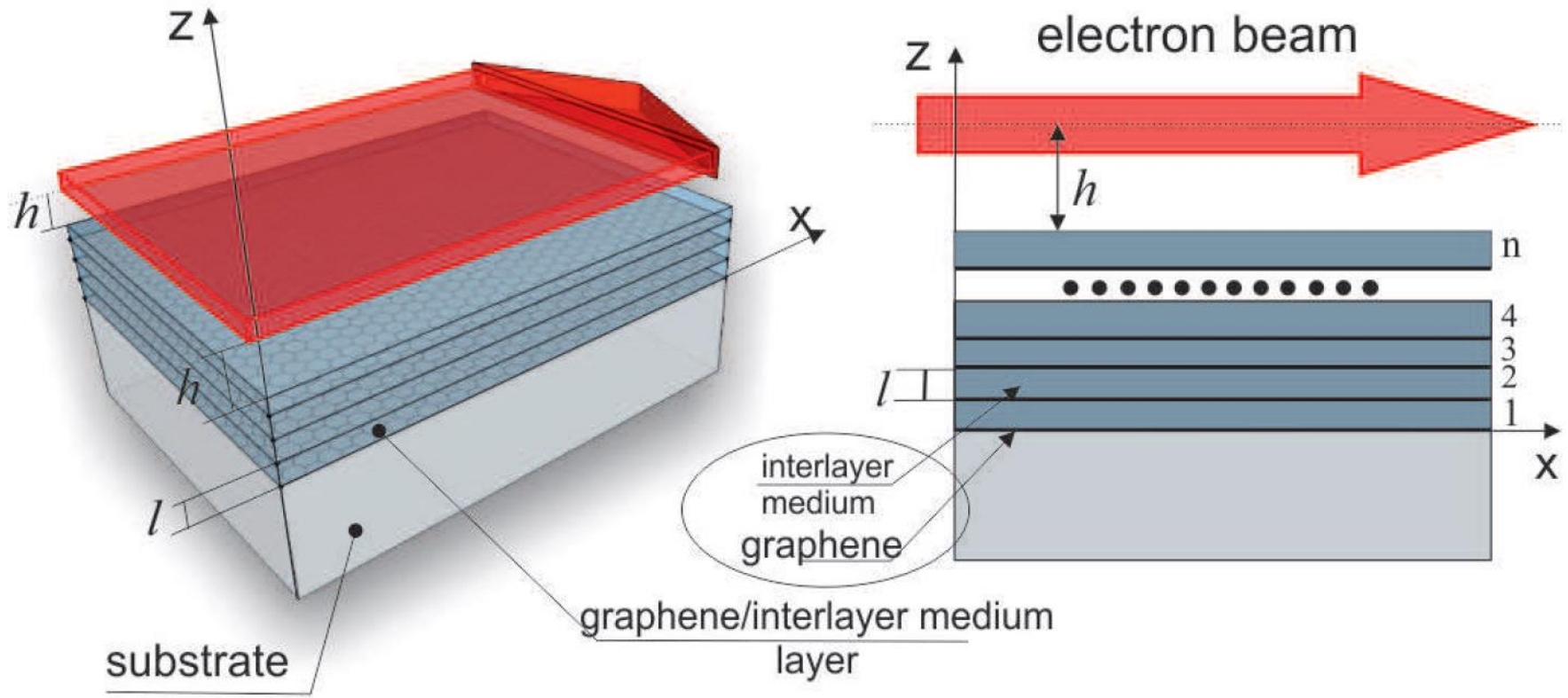

K. Batrakov and S. Maksimenko, Graphene layered systems as a terahertz source with tuned frequency. Phys. Rev. B 95, 205408 (2017)

Generation equation

Continuity conditions on the beam boundaries and discontinuity conditions for magnetic field on graphene layers give dispersion equation for system “sandwich + electron beam” (generation equation)

$$I_b = -\frac{(2+\sigma_0)^2 - (\sigma_0)^2 \exp\{-2\sqrt{q^2-\omega^2/c^2}l\}}{\sigma_0\left[2+\sigma_0+\exp\{-2\sqrt{q^2-\omega^2/c^2}l\}(2-\sigma_0)\right]}$$

Here $\sigma_0 = (4\pi/\omega)k_z\sigma$

$$I_b = \exp(2ik_z h)\frac{(k_{bz}^2-k_z^2)\{\exp(ik_{bz}\delta)-\exp(-ik_{bz}\delta)\}}{(k_{bz}-k_z)^2\exp(ik_{bz}\delta)-(k_{bz}+k_z)^2\exp(-ik_{bz}\delta)}$$

h is distance between sandwich and electron beam, δ is beam thickness,

$$k_{bz} = k_z\sqrt{1-\frac{\omega_l^2}{\gamma^3(\omega-qu)^2}}$$

ω_l is electron beam Langmuir frequency

Instability increments

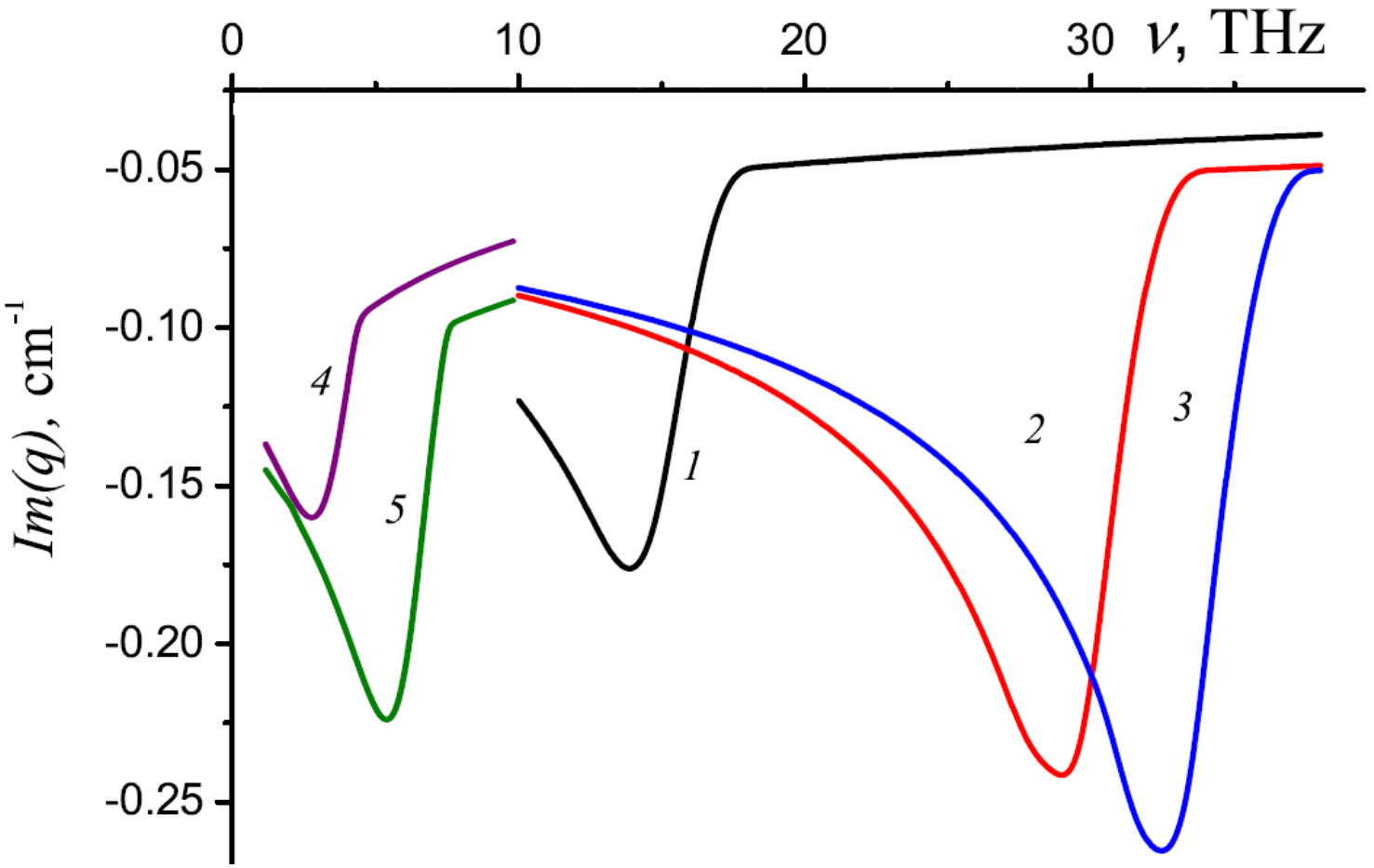

$$\frac{I}{I_0} \sim \exp\{-2\,\mathrm{Im}\,qL\}$$

Frequency dependence of the instability increment $Im(q)$ for 4 (1), 8 (2) and 9 (3) graphene layers with chemical potential of a single layer $\mu = 0.2$ eV. Electron beam energy $E = 10$ keV, $\Gamma = 10$ THz. For comparison, the same dependencies are given for a single graphene layer at the electron beam energy $E = 4$ keV, and chemical potential $\mu = 0.1$ eV (4) and $\mu = 0.2$ eV (5).

Theory and experiment (microwave)

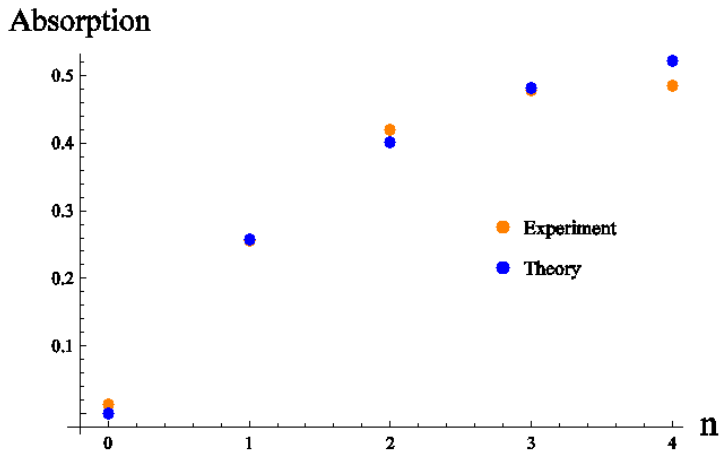

Dependence of absorption on graphene layers numbers ***n*** for "silica+graphene" geometry

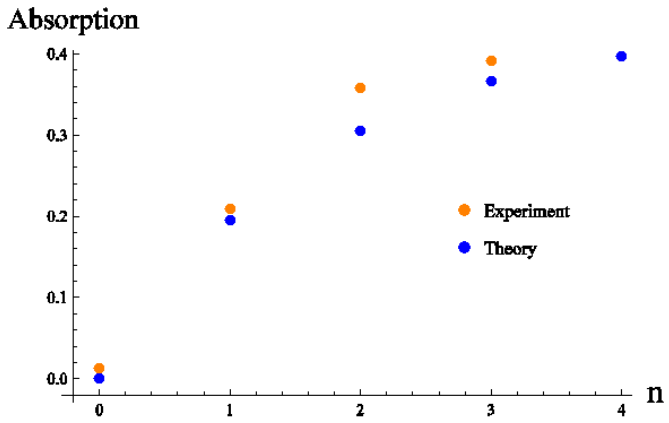

Dependence of absorption on graphene layers numbers ***n*** for "graphene+silica" geometry

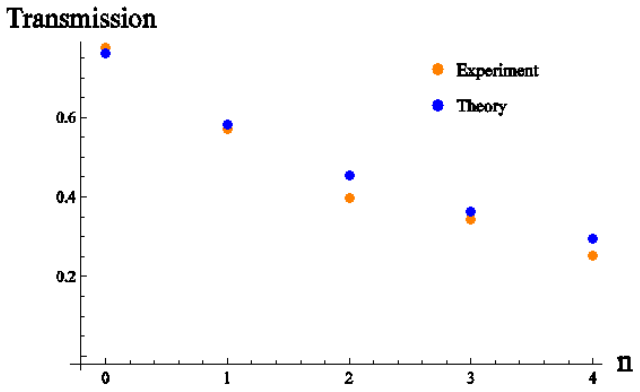

K. Batrakov , P. Kuzhir , S. Maksimenko , A. Paddubskaya , S. Voronovich, Ph Lambin, T. Kaplas & Yu Svirko, *Scientific Reports* **4**, Article number: 7191 (2014)

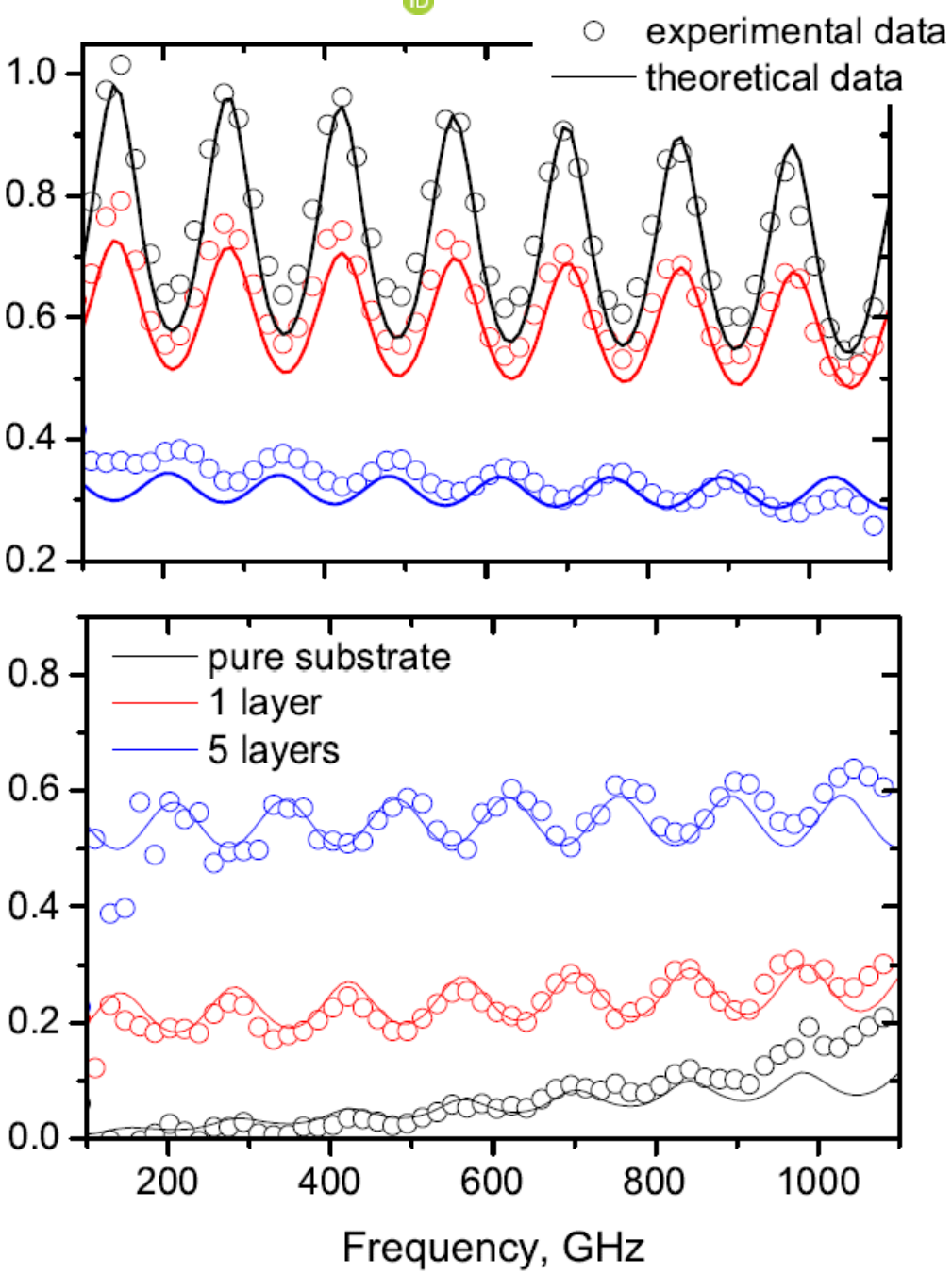

Theory and experiment
(terahertz)

→ transmittance

→ absorbance

K. Batrakov, P. Kuzhir, S. Maksimenko, N. Volynets, S. Voronovich, A. Paddubskaya, G. Valusis, T. Kaplas, Yu. Svirko, *and* Ph. Lambin, Appl. Phys. Lett. **108**, 123101 (2016)

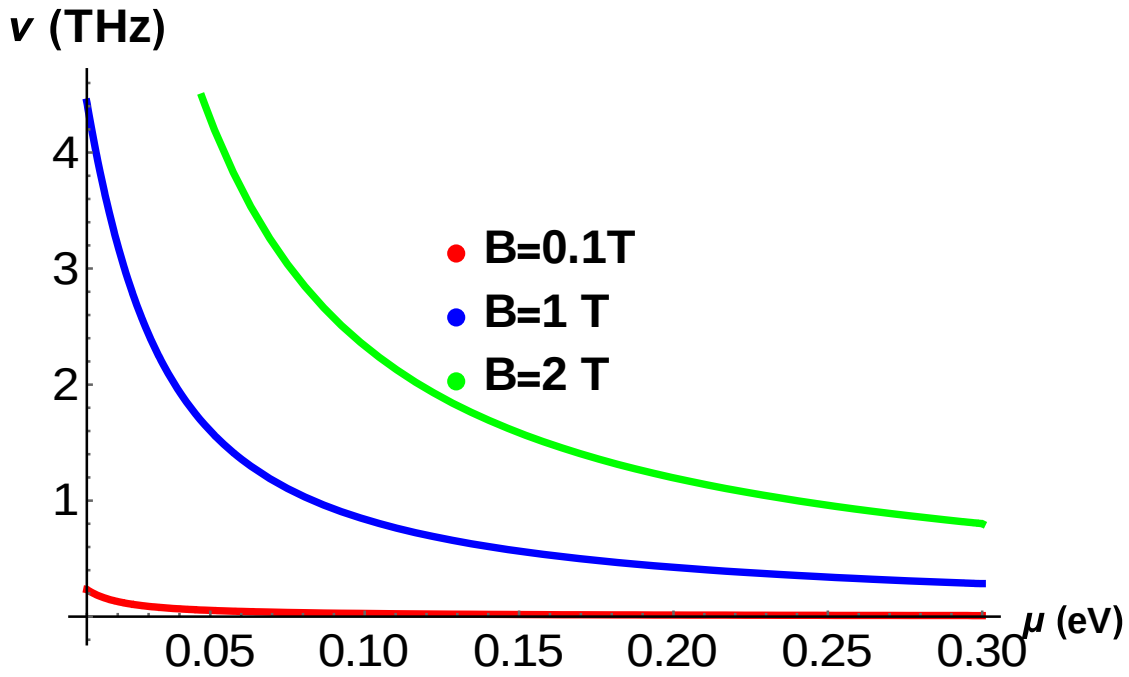

$$\omega_c = \frac{v_F}{l_B}\left(\sqrt{2(N+1)} \pm \sqrt{2N}\right)$$

Here $l_B = \sqrt{\frac{\hbar}{eB}}$ is magnetic length

Dependence of cyclotron resonant frequency due to intraband transitions on chemical potential at different values of magnetic field.

$$\omega_{cross} = \frac{v_F}{l_B}\left(1 - \left(\frac{E}{H}\right)^2\right)^{3/4}\left(\sqrt{2(N+1)} \pm \sqrt{2N}\right) + v_F \frac{E}{H} q$$

RESULTS & CONCLUSION

- Frequency tuning by changing the number of layers in sandwich (symmetric mode);
- Smooth frequency tuning by means of electrostatic doping (electric bias control);
- Change of interlayer distance leads to smooth tuning to electron beam parameters;
- Generation is reachable on the external electron beam, if current density ~ 10 A/cm^2 the length of graphene sheet ~ several cm is needed. In this case the graphene layers in sandwich should not be obligatory whole. In order to provide interaction of the electron beam with the graphene surface wave on the length of several centimeters, it is sufficient to have a mosaic surface comprising disoriented in plane graphene blocks.
- Generation is reachable also on the internal π electron current, but ballistic length should exceed ~several micron that can be realized (???) in high quality nanotubes, graphene or other advance Dirac materials.

Acknowledgments

- U.S. Air Force under Agreement FA9550-15-D-0003,
- Grant Agreement No. 604391 Graphene Flagship
- Project ID 644076 Call H2020-MSCA-RISE-2014 Programme H2020 (CoExAN)
- Belarusian Republican Foundation for Fundamental Research F17ARM-025

Thank you for attention

Frequency tuning by means of electron beam energy

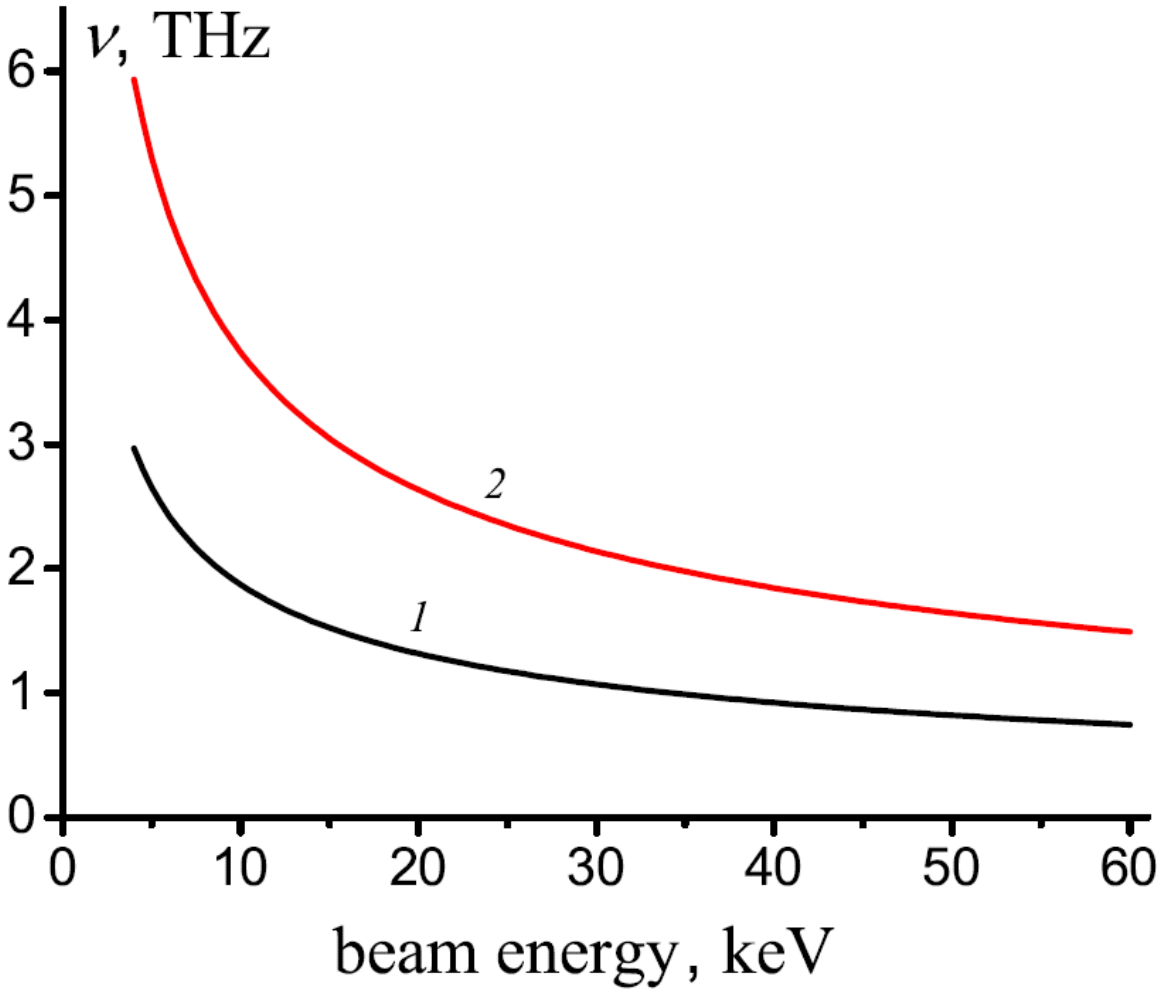

The Čerenkov frequency dependence on the electron beam energy.
Chemical potential 0.1 eV (1) and 0.2 eV (2).

Advantage of using two-wall, multiwall nanotube or graphene for emission

ated wave retardation in single walled nanotube reach 50 times (G. *Slepyan, Lakhtakia, S. Maksimenko*..

long wavelength $\lambda >> d$ (d is the distance between nanotube layers), frequencies may be approximately ten as: $\omega_+ \sim \omega_1(R_1)+\omega_2(R_2)$ and $\omega_- \sim|\omega_1(R_1)-\omega_2(R_2)|$

se velocity corresponding to frequency ω_-, $v_{ph-}=\omega_-/k$ *can be significantly less, than phase velocities esponding to single walled nanotubes* !!! (K. G. Batrakov, P. P. Kuzhir, and S. A. Maksimenko, *Electrical puter Engineering Series archive,Proceedings of the 1st WSEAS international* conference on Nanotechno e of contents,Cambridge, UK,2009, pp. 96–100)

ever $\omega_1(R_1)\neq\omega_2(R_2)$, *therefore decreasing of phase velocity in two-wall nanotube is limited.*

ver graphene has no such drawback?..... But it turns out that phase velocity in bilayer graphene exceeds ph city in graphene monolayer. Electron tunneling

ween graphene layers **is guilty**. Tunneling should be suppressed.

It is realized in spatially separated double-layer or multilayer graphene.

atrakov, V. Saroka, S. Maksimenko, Chr. Thomsen, Journal of Nanophotonics, **6**, 061719 (2012)

Catalytic CVD process

Samples were prepared by Finnish group according to the procedure described in Li, X. et al. Nano Lett. 9, 4359–4363 (2009).

- The first graphene layer was synthesized by chemical vapor deposition (CVD) at 1000 C in methane atmosphere on a copper foil.
- It was next covered by a PMMA layer (poly(methyl methacrylate) is a transparent thermoplastic) obtained by spin coating, after what Cu was wet etched in ferric chloride.
- The obtained PMMA film with its graphene layer was washed in distilled water, placed on a quartz (fused silica) substrate (0.5 mm thickness) and dried.
- The very same procedure was repeated several times, each newly-produced graphene/PMMA unit being deposited on top of the stack obtained at the previous step.

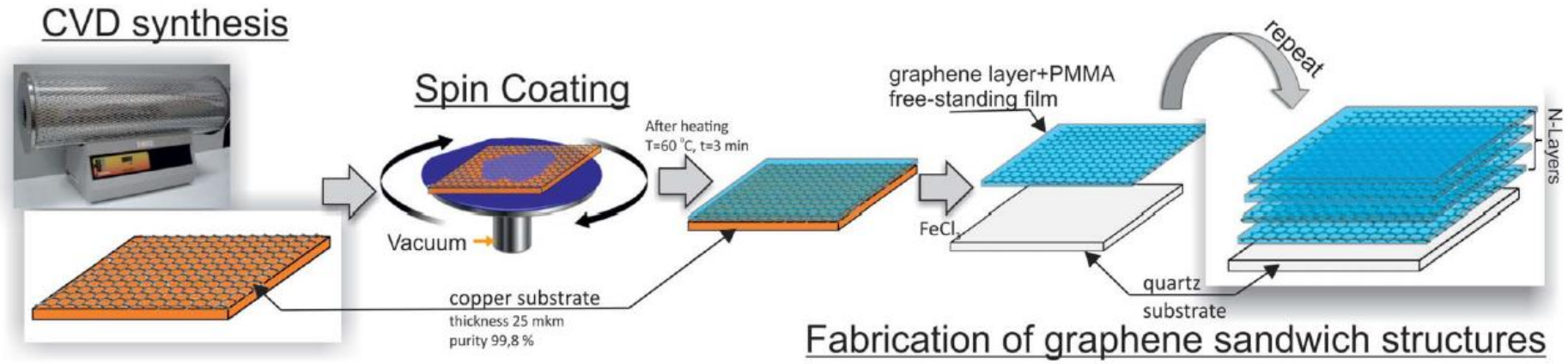

Dispersion equation

$$k - k_m = -\frac{\omega_L^2}{8mk_m c^2} \sum_l B_{nl} \left\{ \frac{1}{-\hbar\omega + \varepsilon_n(p_n) - \varepsilon_l(p_n - \hbar k)} + \frac{1}{\hbar\omega + \varepsilon_n(p_n) - \varepsilon_l(p_n + \hbar k)} \right\}$$

ω_L^2 is Langmuir frequency squared, it proportional to current density.

$$\varepsilon_l(p_n \pm \hbar k) \approx \varepsilon_l(p_n) \pm \hbar k \frac{\partial \varepsilon_l}{\partial p_n} + \frac{\hbar^2 k^2}{2} \frac{\partial^2 \varepsilon_l}{\partial p_n^2}$$

$$v_l = \frac{\partial \varepsilon_l (p_n)}{\partial p_n} \longrightarrow$$ group velocity of nanotube electron

$$\pm\hbar\omega + \varepsilon_n(p_n) - \varepsilon_l(p_n \pm k) = \pm\hbar(\omega - k v_l \pm \Omega_{nl}) + \frac{\hbar^2}{2} \frac{\partial^2 \varepsilon_l}{\partial p_n^2} k^2$$

Typical dispersion equation for second order Cherenkov instability: $k - k_m \sim -\frac{\omega_L^2}{(\omega - k v_l)^2}$

Boundary conditions:

$$E \sim \sum_{i=1}^{3} c_i \exp\left(ik^{(i)}z\right)$$

$$\delta j_n \sim \sum_{i=1}^{3} \frac{c_i}{\nu_i^2} \exp\left(ik^{(i)}z\right)$$

$$\delta j_n - v_n \delta n_e \sim \sum_{i=1}^{3} \frac{c_i}{\nu_i} \exp\left(ik^{(i)}z\right)$$

$$c_1 + c_2 + c_3 = \alpha\left[c_1 \exp\left(ik^{(1)}L\right) + c_2 \exp\left(ik^{(2)}L\right) + c_3 \exp\left(ik^{(3)}L\right)\right]$$

$$\frac{c_1}{\nu_1} + \frac{c_2}{\nu_2} + \frac{c_3}{\nu_3} = 0\,, \qquad \frac{c_1}{\nu_1^2} + \frac{c_2}{\nu_2^2} + \frac{c_3}{\nu_3^2} = 0\,.$$

Threshold current and instability increment of generation

Boundary conditions on nanotube tips and dispersion equations give threshold condition and instability increment

$$\frac{b_{nn}^{(m)}}{v_n^2}\frac{\partial^2\varepsilon_n}{\partial p_n^2}\ L^3\,\frac{x\cos x-\sin x}{x^3}=1-|\alpha|+Lk_m'',$$

$$\omega_m''=\left[\frac{\partial k_m}{\partial\omega}\right]^{-1}\left[\frac{b_{nn}^{(m)}}{v_n^2}\frac{\partial^2\varepsilon_n}{\partial p_n^2}L^2\,\frac{x\cos x-\sin x}{x^3}\right.$$

$$\left.-\frac{1-|\alpha|}{L}-k_m''\right].$$

$x=(\omega-k_m v_n)L/(2v_n)$ - detuning from Cherenkov resonance

MOTIVATION

1) **electromagnetic emitters and sensors as basic elements of developing nano-circuts;**

2) **High need for new THz source with tunable frequency.**